Published in final edited form as:
Cancer Sci. 2011 June ; 102(6): 1216–1222. doi:10.1111/j.1349-7006.2011.01930.x.

Hydroxycamptothecin-Loaded Fe_3O_4 Nanoparticles Induce Human Lung Cancer Cell Apoptosis through Caspase-8 Pathway Activation and Disrupt Tight Junctions

Gen Zhang[1,2], **Lei Ding**[1], **Randall Renegar**[1], **Xue Mei Wang**[2,*], **Qun Lu**[1], **Shouquan Huo**[3], and **Yan-Hua Chen**[1,*]

[1] Department of Anatomy and Cell Biology, Brody School of Medicine, East Carolina University, Greenville, NC 27834, USA

[2] State Key Laboratory of Bioelectronics (Chien-Shiung Wu Laboratory), Department of Biological Science and Medical Engineering, Southeast University, Nanjing, 210096, P. R. China

[3] Department of Chemistry, East Carolina University, Greenville, NC 27834, USA

SUMMARY

10-Hydroxycamptothecin (HCPT) elicits strong anti-cancer effects and is less toxic making it widely used in recent clinical trials. However, its low solubility limits its application as an effective anti-cancer therapy. In this study, we investigate the hypothesis that the unique water dispersible oleic acid-Triton X-100-coated Fe_3O_4 nanoparticles loaded with HCPT disrupt epithelial cell-cell junctions and induce human lung cancer cell apoptosis through caspase-8 pathway. We characterized the HCPT-loaded nanoparticles and determined their effects on lung cancer cell viability and apoptosis by using immunofluorescence light microscopy and SDS-PAGE/immunoblots. We found that HCPT-loaded nanoparticles elicited an anti-proliferative effect in a dose-dependent manner. HCPT-loaded nanoparticles reduced the expression of cell-cell junction protein claudins, E-cadherin, and ZO-1, and transmission electron microcopy demonstrated a disrupted tight junction ultrastructure. Transepithelial electric resistance was also reduced indicating the reduction of tight junction functions. HCPT increased phosphorylation of p38 and SAPK/Jun kinase while it showed no effects on p42/44 MAP kinase. Compared with void Fe_3O_4 nanoparticles or HCPT drug alone, HCPT drug-loaded nanoparticles evoked synergistic effects by increasing cell apoptosis with enhanced activation of caspase-8 pathway. Therefore, our current study highlights the potential of HCPT drug-loaded nanoparticles as a chemotherapeutic agent for increasing anti-cancer drug efficacy.

Keywords

Nanoparticles; anti-cancer drug; apoptosis; HCC827 cells; caspase-8; tight junctions

[*]Author for Correspondence: Yan-Hua Chen, Department of Anatomy and Cell Biology, East Carolina University Brody School of Medicine, Greenville, NC 27834; Tel: 252-744-1341 Fax: 252-744-2850, cheny@ecu.edu. Xue Mei Wang, State Key Lab of Bioelectronics (Chien-Shiung Wu Lab), Department of Biological Science and Medical Engineering, Southeast University, Nanjing, 210096 P. R. China, Tel: 025-83792177, xuewang@seu.edu.cn.

DISCLOSRE SATEMENTS

The authors have no financial interests in or financial conflict with the subject matter discussed in this manuscript.

INTRODUCTION

Camptothecin (CPT) is a natural alkaloid extracted from the Chinese tree, Camptotheca *Acuminata Decne*. Due to its potent anti-cancer activity, CPT and its derivatives have received increasing attention in recent years. The anti-tumor mechanism of these compounds is based on the inhibition of DNA replication and RNA transcription by stabilizing the cleavable complexes formed between topoisomerase I (topo I) and DNA. The complex formation prevents DNA re-ligation and causes DNA damage which results in apoptosis.[1] Among its analogues, 10-Hydroxycamptothecin (HCPT) shows strong anti-tumor effects and is less toxic compared to CPT. HCPT has been widely used in the treatment of a variety of cancers in clinical trials. [2]Unfortunately, HCPT has poor solubility in physiologically acceptable solvents and is usually used in the more soluble carboxylate salt form that is more toxic and less active. [2]

Nanotechnology offers promising applications in cancer treatments due to the unique properties of nanostructures. Drug-coated polymer nanoparticles could efficiently increase the intracellular accumulation of anti-cancer drugs. [3] One emerging application is to use surface modified Fe_3O_4 magnetic nanoparticles as vehicles for drug delivery. [4] However, relatively high toxicity of uncoated magnetic nanoparticles restricts their use in humans. Therefore, many approaches have focused on the encapsulation of magnetic nanoparticles with biocompatible materials to reduce toxicity. [5, 6] Triton X-100, a derivative of polyethylene glycol (PEG), is widely used in biological applications due to its low toxicity and good biologic compatibility.[7] Recently, Paciotti et al reported a water-dispersible oleic acid (OA)-Pluronic-coated iron oxide nanoparticle formulation that can be loaded easily with high doses of water-insoluble anti-cancer agents. [4]

The nanocomposites of polylactide (PLA) nanofibers and tetraheptylammonium-capped Fe_3O_4 magnetic nanoparticles have been tested using a different anti-cancer drug daunorubicin, [3, 8] which can inhibit tumor growth. [9] The nanoparticles composed of chitosan/poly-γ-glutamic acid could affect tight junction (TJ) function. [10] However, the feasibility of Fe_3O_4 magnetic nanoparticles loaded with HCPT in the presence of Triton X-100 has not been investigated. There are significant interests to reveal whether this nanoparticle based technology coupled with HCPT can induce cancer cell death through well-characterized molecular and cellular signaling mechanisms.

To overcome these limitations, we have developed an efficient delivery system that utilizes Fe_3O_4 magnetic nanoparticles loaded with a high dose of HCPT in the presence of Triton X-100. We report that HCPT drug-loaded nanoparticles induce apoptosis in human lung cancer HCC827 cell line, as determined by molecular, biochemical, and morphological methods. We find that nanoparticles and HCPT drug-loaded nanoparticles disrupt TJs and increase the permeability of epithelial monolayers. Furthermore, we demonstrate that the cancer cell inhibitory effects induced by HCPT drug-loaded nanoparticles involve the activation of caspase-8 as well as p38 and SAPK/Jun kinase signaling pathways.

MATERIALS AND METHODS

Preparation of magnetic Fe_3O_4 nanoparticles and drug-loaded nanoparticles

$FeCl_3$ was suspended in dH_2O under a nitrogen-gas atmosphere to remove oxygen from the mixture followed by addition of $FeCl_2$ to the mixture. Ammonia solution was added drop wise with stirring until the mixture had a pH 9.0–10.0. The particles obtained were washed with nitrogen purged water. Oleic acid (OA) was added to the above solution of particles. The mixture was stirred at 80°C to evaporate the ammonia and then cooled to room temperature. Triton X-100 was added to the OA-coated nanoparticles, and the suspension

was stirred overnight. HCPT dissolved in DMSO was added to the aqueous dispersion of OA-Triton X-100-stabilized Fe_3O_4 nanoparticles. The mixture underwent stirring overnight in a nitrogen-gas atmosphere to allow partitioning of the drug into the OA shell surrounding Fe_3O_4 nanoparticles. Drug-loaded nanoparticles (HTOFN) were washed and separated from the unentrapped drug using a magnet.

Transmission Electron Microscopy

The HTOFN were observed under the transmission electron microscopy (TEM) and the samples for analysis were prepared by applying the diluted suspensions onto carbon-coated copper grids and allowing the solvent to evaporate.

To investigate the effects of HTOFN on cell-cell junctions, HCC827 cells were incubated with HTOFN and then fixed in 2.5% glutaraldhyde. Ultrathin sections were viewed under a JEOL 1200-EX transmission electron microscope and images were taken using a MegaView III CCD camera and ITEM imaging software.

X-Ray Diffraction

The HTOFN were characterized by X-ray powder diffraction (XRD) (D/Max-IIIC, Japan) using Co K[alpha] radiation: 1.789Å. Distances between peaks were compared to the information related for diffraction data to determine crystalline structures.

Cell Culture and MTT Assay

HCC827 (human non-small cell lung cancer) cells from American Type Culture Collection (ATCC, Manassas, VA) were grown in RPMI 1640 medium supplemented with 10% fetal bovine serum (Gibco BRL, Grand Island, NY) at 37°C in a humidified air-5% CO_2 atmosphere.

For cytotoxicity analysis, MTT assays were performed on cells treated with various concentrations of HTOFN, void nanoparticles (TOFN), and HCPT (dissolved in DMSO with the final concentration 0.2%). The optical density (OD) was read at a wavelength of 540 nm. All experiments were performed in triplicates. Relative inhibition of cell growth was expressed as follows: % cell growth inhibition = (1−[OD]test/[OD]control)×100%.

Apoptosis Measurements

Apoptotic DNA was extracted from the HCC827 cells using Apoptotic DNA ladder Isolation Kit (BioVision). The DNA ladders were stained with ethidium bromide and DNA fragmentation was visualized under UV light.

Apoptotic cells were also determined by FACSCalibur Flow Cytometer (BD Biosciences) using Annexin-V-FITC Apoptosis Detection Kit (Calbiochem).

In addition, HCC827 cells were stained with acridine orange dye mix and viewed using a fluorescence microscope. All experiments were repeated three times and a total of 200 cells were counted for each experiment.

Intracellular HCPT Measurement

To measure intracellular HCPT accumulation, HCC827 cells treated with HTOFN or HCPT were harvested and lysed with DMSO. The cell extracts were sonicated and centrifuged, and the supernatant was then loaded onto HPLC for analysis.

Electrophoresis and Immunoblotting

HCC827 cells lysed in RIPA buffer were subjected to SDS-PAGE/immunoblot analysis. The primary antibodies, occludin, claudin-1, claudin-2, claudin-3, claudin-4, claudin-7, ZO-1, and E-cadherin were obtained from Zymed (Invitrogen, Carlsbad, CA) while all other antibodies were purchased from the Cell Signaling Technologies (Danvers, MA). The proteins were detected by enhanced chemiluminescence (GE Healthcare, NJ).

Immunofluorescence Light Microscopy

After various treatments, HCC827 cells were fixed in cold methanol and were incubated with primary antibodies followed by incubation with secondary antibodies. The fluorescent signal was analyzed using a Zeiss AXIO IMAGER M1 microscope (Carl Zeiss MicroImaging, Inc., Thornnwood, NY).

Measurement of Transepithelial Electrical Resistance

HCC827 cells were plated on Transwell inserts and treated with HTOFN or TOFN. Transepithelial electrical resistance (TER) was determined by a Millicell-ERS voltohmmeter (Millipore Corp., Bedford, MA). [11] All TER values were calculated by subtracting the resistance measured in the blank insert from the resistance measured in the insert with the monolayer and then multiplied by the surface area of the membrane. All experiments were repeated three times and the data were shown as the means ± SEM with asterisk indicating $P < 0.05$.

RESULTS

HCPT drug-loaded Fe_3O_4 nanoparticles

We applied the unique water dispersible oleic acid-Triton X-100-coated Fe_3O_4 nanoparticles to load with HCPT. Transmission electron microscopy (TEM) demonstrated the images of the successful drug-loaded nanoparticles (HTOFN) at low (*a*) and high (*b*) resolution, respectively (Fig 1A). The average size of HTOFN is about 14 nm. Figure 1A (*b*) shows the presence of a crystalline structure within the HTOFN core. X-ray Diffraction (XRD) further demonstrated the XRD spectra of HTOFN (Fig 1B), and no peak of impurity was observed, indicating that no new phases were formed and the crystalline structure of magnetite Fe_3O_4 nanoparticles did not change during the drug loading production. The peaks agreed with the standard Fe_3O_4 (cubic phase) XRD spectrum [12] and confirmed that the HTOFN cores were magnetite. Other methods such as Fourier Transform Infrared (FT-IR) spectroscopy and HPLC also provided quality assessment of the HCPT drug-loaded Fe3O4 nanoparticles (See supplemental materials and Fig S1 for details).

Increased cell apoptosis induced by HCPT drug-loaded Fe_3O_4 nanoparticles

To determine whether HTOFN can increase the anti-cancer drug efficacy and promote cell death, we performed cytotoxicity assays using the human lung cancer cell line HCC827. The concentration of HCPT used to treat HCC827 cells was the same as that loaded in HTOFN. Under these experimental conditions, HTOFN significantly inhibited the cell growth compared with HCPT treatment (Fig. 2A, HTOFN and HCPT). In addition, HTOFN demonstrated a sustained, dose-dependent anti-proliferative activity in HCC827 cells. Nanoparticles alone also had some effects in inhibiting cell growth compared with that of HCPT alone (Fig. 2A, TOFN and HCPT).

To determine whether the cell growth inhibition was due to the apoptotic response, the DNA fragmentations were examined by agarose gel electrophoresis. When HCC827 cells were treated with HTOFN, the intensity of fragmented chromosomal DNA bands was much

higher than that observed from cells treated with TOFN or HCPT (Fig. 2B, lane 1, 2, and 3, respectively). The formation of DNA ladders was clearly present after treatment with TOFN, but only weakly discernible when the cells were treated with HCPT. These results provide the evidence that the remarkable enhancement of apoptosis was induced by the synergistic effect of Fe_3O_4 nanoparticles with HCPT in HTOFN on HCC827 cells.

Flow cytometry assays were carried out to verify the results obtained from DNA fragmentation experiments. Figure 2C shows that using Annexin-V-FITC apoptosis detection method, HTOFN induced a much higher cell apoptosis rate than that of TOFN, HCPT, or untreated control. We also observed an increase in the number of apoptotic nuclei in the HCC827 cells treated with HTOFN (Fig. 3A). Using acridine orange staining for apoptotic cells, apoptotic nuclei were identified by their distinctively marginated and fragmented appearance under the fluorescent microscope. We found that the percentage of apoptotic cells was 65.2%, 33.4%, or 8.9% for HTOFN, TOFN, or HCPT treatment, respectively (Fig. 3B). In summary, each of these experiments demonstrated a substantial increase in cell apoptosis following treatment of HCC827 cells with HTOFN.

Intracellular accumulation of HCPT

Drug-loaded nanoparticles (HTOFN) clearly inhibited cell growth and increased the cell apoptosis. To understand the potential mechanism of this effect, HPLC was used to measure HCPT concentrations in HCC827 cells (Fig. 4). Our experimental results revealed that the concentration of HCPT was much higher in HTOFN-treated cells (Fig. 4D, peak 1) compared with that of TOFN or HCPT-treated cells (Fig. 4C and E, peak 1). Figure 4F showed that the accumulation of HCPT in HTOFN-treated cells was 58% of the HCPT (8.6×10^{-1} mg/L) loaded in HTOFN while the accumulation of HCPT in HCPT-treated cells was only 15% of 8.6×10^{-1} mg/L HCPT (the treatment dosage). These results indicate that HTOFN facilitated the uptake of the drug into HCC827 cells.

Activation of the caspase-8 pathway by HCPT drug-loaded Fe_3O_4 nanoparticles

To further explore the molecular mechanisms underlying the HTOFN-mediated apoptosis in HCC827 cells, we investigated apoptosis-related protein expression in HCC827 cells. When HCC827 cells were treated with HTOFN, the cleaved caspase-8 (p43/p41) signals on western blots were much stronger than those for cells treated with TOFN or HCPT alone (Fig. 5A). Similar results were obtained for cleaved caspase-9 and caspase-3. Poly (ADP-ribose) polymerase (PARP) is a known downstream target of active caspase-3 and can be cleaved during the induction of apoptosis. In HCC827 cells treated with HTOFN or TOFN, the cleavage of PARP via the proteolytic degradation of a full length PARP into the activated form was detected along with caspase-3 activation. Treatment of cells with HCPT at the concentration that was loaded in HTOFN did not initiate the activation of PARP above the control level (Fig. 5A). These data suggest that HTOFN treatment induces cell apoptosis by increasing activation of caspase-8 pathway in HCC827 cells. Figure 5B summarizes the HTOFN-induced cell apoptosis activation signaling pathway.

Effects of HCPT drug-loaded Fe_3O_4 nanoparticles on cell-cell junction integrity

Functional cell-cell junction indicates the epithelial cell integrity. We first examined the subcellular distribution of TJ proteins by immunofluorescence light microscopy. In untreated epithelial cell monolayers, TJ integral membrane proteins, such as claudin-1, -3, -4, -7, and occludin as well as TJ associate protein ZO-1, were all localized at the cell-cell junction (Fig 6, Control). The adherens junction marker, E-cadherin, was also concentrated at the cell-cell contact area. However, in HTOFN or TOFN-treated cell monolayers, all of the above proteins except occludin were internalized and the immunostaining signals were either reduced or disrupted (Fig. 6, HTOFN and TOFN).

We also examined TJ ultrastructure by TEM on HTOFN or TOFN-treated cells. In control HCC827 cells, the TJ was observed at the apical surface of adjacent cells as expected (Fig. 7A: a). However, TJ structure was often absent in the cells treated with HTOFN or TOFN (Fig. 7A: b and c).

To determine whether the TJ function had been affected, we measured the TER, a well-established method to assay the TJ barrier function of an epithelial monolayer. Our results revealed that TER was significantly decreased in the cell monolayers treated with HTOFN or TOFN, indicating that Fe_3O_4 nanoparticles reduced TJ barrier function (Fig. 7B).

We finally sought to determine the expression of cell-cell junction proteins and the proteins of MAP kinase signaling pathways that are known to regulate cell-cell junctions in epithelial cells. The protein expression levels of claudin-1, -3, -4, -7, ZO-1, and E-cadherin were all decreased in a dose-dependent manner in the cells treated with HTOFN or TOFN (Fig. 8A). Claudin-2 was not expressed in HCC827 cell (data not shown). Interestingly, there was no significant change in the protein expression level of occludin after HTOFN or TOFN treatment, consistent with the subcellular localization result shown in Figure 6. Finally, we examined the signaling pathway changes after treatment with HTOFN or TOFN.

Among the MAP kinase family members, p38 MAP kinase was potently activated in a time-dependent fashion in HTOFN or TOFN-treated cells (Fig. 8B). The stress-activated protein kinase/Jun-amino-terminal kinase (SAPK/JNK) was also activated by HTOFN or TOFN treatment. In contrast, the phosphorylation of ERK1/ERK2 did not change following treatments, suggesting that the effects of treatments were potentially through the p38 or SAPK/JNK, but not through the activation of the ERK1/ERK2 MAP kinase signaling pathway.

DISCUSSION

In this study, we have characterized a newly developed water-dispersible Fe_3O_4 nanoparticle-based formulation that can be loaded efficiently with the water-insoluble anti-cancer drug HCPT, a CPT analogue. The HCPT-loaded nanoparticles (HTOFN) demonstrated anti-proliferative activity in human lung cancer cells and also induced cell apoptosis through the activation of caspase-8 pathway.

Previously, the drug and nanoparticles were either conjugated chemically through the covalent bond or formed the bond through ionic interactions. However, the formation of the covalent bond may result in the difficulty of drug release while the binding through ionic interactions can result in the drug dissociation from nanoparticles during the process of synthesis. In our nanomaterials, Fe_3O_4 nanoparticles were surrounded by the OA shell while Triton X-100 was anchored at the OA-water interface (Fig. S1). HCPT was loaded between the OA shell and Triton X-100. This formulation could offer greater flexibility in terms of loading of water-insoluble drug HCPT as well as for efficient drug release. Our results indicated that OA is chemisorbed as a carboxylate headgroup on the surface of Fe_3O_4 nanoparticles. Thus it is expected to provide better association of drug to nanoparticles with the surrounding OA shell acting as a drug reservoir. The OA shell can also protect Fe_3O_4 nanoparticles from oxidation and/or hydrolysis in the presence of water, which can significantly reduce the magnetization of the Fe_3O_4 nanoparticles.[4]

Triton X-100 is a nonionic detergent that is often used in biochemical applications to solubilize proteins. [13] We propose that the hydrophobic segments of Triton X-100 anchor at the interface of the OA shell around Fe_3O_4 nanoparticles and the hydrophilic segments extend into the aqueous phase (Fig. S1). The OA shell surrounding the Fe_3O_4 nanoparticles plays the dual role serving as a drug reservoir as well as an interface for anchoring the

hydrophobic chains of Triton X-100 to make the formulation water-dispersible. Therefore, this formulation could facilitate the entry of an anti-cancer drug into cancer cells and enhance the accumulation of relevant molecules in the target cells. [14] Consistent with this hypothesis, results from our current study showed that the concentration of HCPT was significantly higher in HTOFN-treated cells than in HCPT-treated cells.

Apoptosis is an important biological process in many systems and can be triggered by a variety of stimuli. [15] The caspase-family represents the key components of the apoptotic machinery within the cells and consists of at least 14 different caspase proteases in mammals. [16] Our results demonstrated that HTOFN treatments efficiently inhibited HCC827 cell growth and greatly increased cell apoptosis. When cells were treated with HTOFN, they exhibited morphological features characteristic of apoptosis, such as membrane shrinkage and chromosomal condensation. Although some previous studies reported that nanoparticles could induce cell apoptosis, the underlying molecular mechanism was unclear. [17, 18] We found that HTOFN treatments activated caspase-8 pathway to induce apoptosis in HCC827 cells. Cleaved caspase-8 activated caspase-3 and caspase-9 that correlated with the increased cleaved PARP expression after HTOFN treatments. Although TOFN could also induce the activation of caspase-8 pathway compared to HCPT treatments and the control without treatment, the effects of TOFN alone on apoptosis were quite moderate when compared to that of HTOFN.

TJ is the most apical component of the junctional complex in epithelial and endothelial cells and separates the apical from the basaolateral membrane and restricts the diffusion of ions and small molecules through the paracellular pathway. [19] It is well known that cell junctions are critical for maintaining normal epithelial cell functions and cell survival. [20] We found that HTOFN and TOFN disrupted TJs and the barrier function by down-regulation of TJ as well as adherens junction protein expression. The localization of cell junction proteins was changed from cell membrane to the cytoplasm after HTOFN and TOFN treatments. The reduced expression of TJ proteins was correlated with a significantly increase in phosphorylation of p38 MAP kinase and SAPK/JNK in a time-dependent manner. The effect of TOFN on TJ disruption and p38 activation is most likely due to the oleic acid coated on TOFN since oleic acid has been reported to decrease TER and the barrier function, disrupt cell-cell contacts as well as activate the p38 MAPK. [21, 22] Taking together, we propose that HTOFN and TOFN-induced TJ disruption is mediated through the activation of p38 and stress-related signaling pathways.

Supplementary Material

Refer to Web version on PubMed Central for supplementary material.

Acknowledgments

We thank Rodney Tatum, Beverly G. Jeansonne, and Joani T. Zary for their technical assistance. This research was supported in part by the National Institutes of Health Grants ES016888 and HL085752 (YHC), CA111891 (QL), and from the grants of the National Natural Science Foundation of China (90713023) and National Basic Research Program of China (2010CB732404) (XMW).

References

1. Wall ME, Wani MC, Cook CE, et al. Plant antitumor agent.1. The isolation and structure of camptothecin, a novel alkaloidal leukemia and tumor inhibitor from camptotheca acumianta. J Am Chem Soc. 1966; 88:3888–90.
2. Pu X, Sun J, Wang Y, et al. Development of a chemically stable 10-hydroxycamptothecin nanosuspensions. Int J Pharm. 2009; 379:167–73. [PubMed: 19505545]

3. Lv G, He F, Wang X, et al. Novel nanocomposite of nano fe(3)o(4) and polylactide nanofibers for application in drug uptake and induction of cell death of leukemia cancer cells. Langmuir. 2008; 24:2151–6. [PubMed: 18193905]
4. Jain TK, Morales MA, Sahoo SK, et al. Iron oxide nanoparticles for sustained delivery of anticancer agents. Molecular Pharmaceutics. 2005; 2:194–205. [PubMed: 15934780]
5. Kwon HY, Lee JY, Choi SW, et al. Preparation of PLGA nanoparticles containing estrogen by modified emulsification-diffusion method. Coll Surf A. 2001; 182:123–30.
6. Lemoine D, Francois C, Kedzierewicz F, et al. Stability study of nanoparticles of poly(epsilon-caprolactone), poly(D,L-lactide) and poly(D,L-lactide-co-glycolide). Biomaterials. 1996; 17:2191–97. [PubMed: 8922605]
7. Guo R, Wei P, Liu W. Combined antioxidant effects of rutin and vitamin C in Triton X-100 micelles. J Pharm Biomed Anal. 2007; 43:1580–6. [PubMed: 17196356]
8. Gibson JD, Khanal BP, Zubarev ER. Paclitaxel-functionalized gold nanoparticles. J Am Chem Soc. 2007; 129:11653–61. [PubMed: 17718495]
9. Blanco E, Bey EA, Khemtong C, et al. Beta-lapachone micellar nanotherapeutics for non-small cell lung cancer therapy. Cancer Res. 2010; 70:3896–904. [PubMed: 20460521]
10. Lin YH, Chung CK, Chen CT, et al. Preparation of nanoparticles composed of chitosan/poly-gamma-glutamic acid and evaluation of their permeability through Caco-2 cells. Biomacromolecules. 2005; 6:1104–12. [PubMed: 15762683]
11. Alexandre MD, Lu Q, Chen YH. Overexpression of claudin-7 decreases the paracellular Cl− conductance and increases the paracellular Na+ conductance in LLC-PK1 cells. J Cell Sci. 2005; 118:2683–93. [PubMed: 15928046]
12. Daou TJ, Buathong S, Ung D, et al. Investigation of the grafting rate of organic molecules on the surface of magnetite nanoparticles as a function of the coupling agent. Sensors and Actuators B-Chemical. 2007; 126:159–162.
13. Sorger H, Kretschmer K, Aurich H. Temperature dependence of membrane-bound aldehyde dehydrogenase from Acinetobacter: effect of solubilization and chain length of the substrates. Biomed Biochim Acta. 1986; 45:315–9. [PubMed: 3707551]
14. Guo D, Wu C, Li X, Jiang H, Wang X, Chen B. In vitro cellular uptake and cytotoxic effect of functionalized nickel nanoparticles on leukemia cancer cells. J Nanosci Nanotechnol. 2008; 8:2301–7. [PubMed: 18572641]
15. Vier J, Gerhard M, Wagner H, Hacker G. Enhancement of death-receptor induced caspase-8-activation in the death-inducing signalling complex by uncoupling of oxidative phosphorylation. Mol Immunol. 2004; 40:661–70. [PubMed: 14644092]
16. Wang Y, Gu X. Functional divergence in the caspase gene family and altered functional constraints: statistical analysis and prediction. Genetics. 2001; 158:1311–20. [PubMed: 11454777]
17. Ding J, Tao K, Li J, Song S, Sun K. Cell-specific cytotoxicity of dextran-stabilized magnetite nanoparticles. Colloids Surf B Biointerfaces. 2010; 79:184–90. [PubMed: 20427159]
18. Hua MY, Yang HW, Chuang CK, et al. Magnetic-nanoparticle-modified paclitaxel for targeted therapy for prostate cancer. Biomaterials. 2010; 31:7355–63. [PubMed: 20609471]
19. Gonzalez-Mariscal L, Betanzos A, Nava P, Jaramillo BE. Tight junction proteins. Prog Biophys Mol Biol. 2003; 81:1–44. [PubMed: 12475568]
20. Ju Y, Wang T, Li Y, Xin W, Wang S, Li J. Coxsackievirus B3 affects endothelial tight junctions: possible relationship to ZO-1 and F-actin, as well as p38 MAPK activity. Cell Biol Int. 2007; 31:1207–13. [PubMed: 17544707]
21. Deli MA. Potential use of tight junction modulators to reversibly open membranous barriers and improve drug delivery. Biochimica et Biophysica Acta. 2009; 1778:892–10. [PubMed: 18983815]
22. Yamasaki M, Tachibana H, Yamada A, Ochi Y, Madhyastha H, Nishiyama K, Yamada K. Oleic acid prevents apoptotic cell death induced by *trans*10, *cis*12 isomer of conjugated linoleic acid via p38 MAP kinase dependent pathway. In Vitro Cell Dev Biol Animal. 2008; 44:290–4.

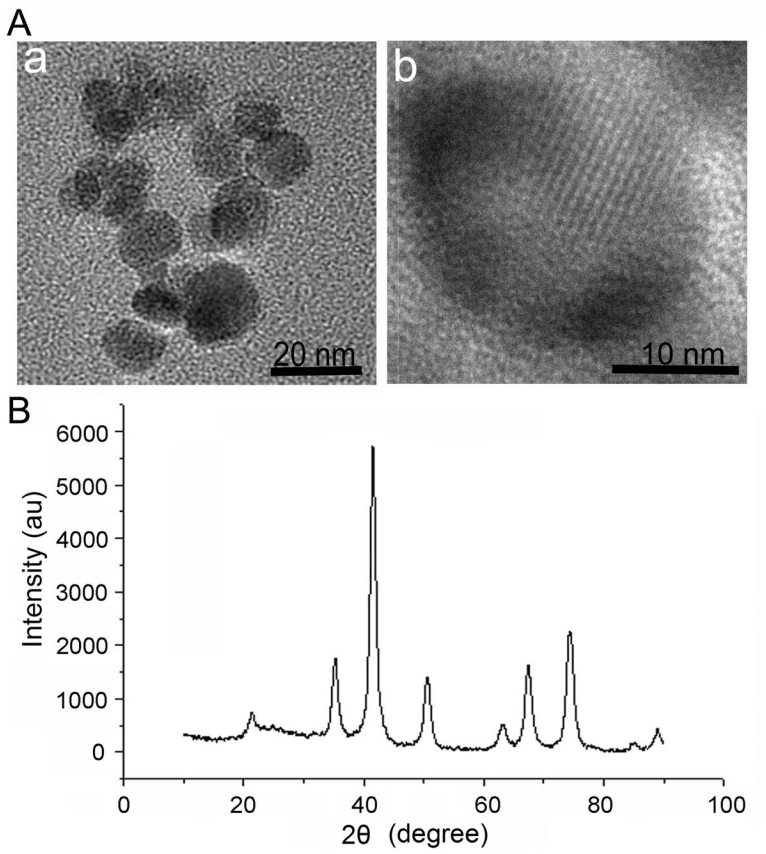

Figure 1.

The characterization of HCPT-loaded nanoparticles (HTFON). **A.** The transmission electron microscopy (TEM) images of HTOFN. **(a)** TEM image of HTOFN at the low magnification. **(b)** TEM image of an individual nanocrystal of HTOFN at the high resolution. **B.** HTOFN was characterized by X-ray diffraction. The peak represents the crystalline structure of Fe_3O_4 nanoparticles. au: artificial units.

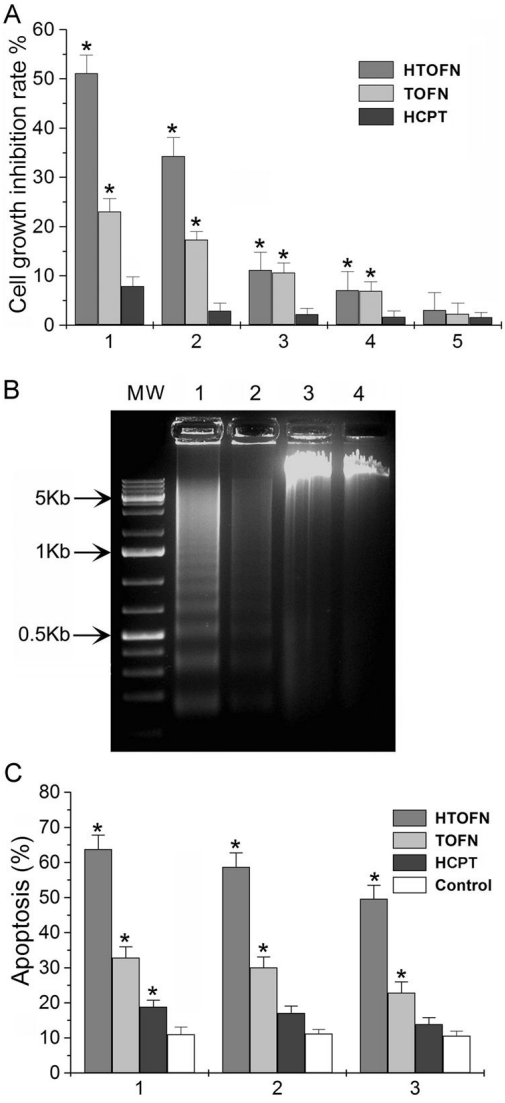

Figure 2.

Increased growth inhibition and apoptosis induced by HTOFN treatments in HCC827 cells. **A.** HCC827 cells were treated with (1) 10 mg/L HTOFN, 10 mg/L TOFN, 8.6×10^{-2} mg/L HCPT; (2) 1 mg/L HTOFN, 1 mg/L TOFN, 8.6×10^{-3} mg/L HCPT; (3) 0.1 mg/L HTOFN, 0.1 mg/L TOFN, 8.6×10^{-4} mg/L HCPT; (4) 0.01 mg/L HTOFN, 0.01 mg/L TOFN, 8.6×10^{-5} mg/L HCPT; (5) 0.1×10^{-2} mg/L HTOFN, 0.1×10^{-2} mg/L TOFN, 8.6×10^{-6} mg/L HCPT. The treatment time was 36 hours. * $P < 0.05$, compared to the HCPT treatment. **B.** The genomic DNA was isolated from the HCC827 cells that underwent various treatments. The DNA ladders were visualized under UV light. Lane M: Molecular weight markers; Lane 1: Cells treated with 10 mg/L HTOFN; Lane 2: Cells treated with 10 mg/L TOFN; Lane 3: Cells treated with 8.6×10^{-2} mg/L HCPT at the concentration that was loaded in 10 mg/L HTOFN; Lane 4: DNA isolated from HCC827 cells without any treatment. **C.** Increased apoptosis after HTOFN treatments for 36 hours. The apoptotic cells were detected by Flow Cytometry using Annexin-V-FITC method. HCC827 cells were treated with 10 mg/L HTOFN, 10 mg/L TOFN, 8.6×10^{-2} mg/L HCPT (1), or with 1 mg/L HTOFN, 1 mg/L TOFN, 8.6×10^{-3} mg/L HCPT (2), or with 0.1 mg/L HTOFN, 0.1 mg/L TOFN, 8.6×10^{-4}

mg/L HCPT (3). White columns indicate the control without treatment. * $P < 0.05$, compared to the control.

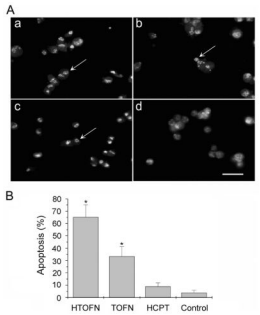

Figure 3.

Detection of apoptotic cells by Acridine Orange Staining. **A.** HCC827 cells were treated with 10 mg/L HTOFN (**a**), 10 mg/L TOFN **(b**), 8.6×10^{-2} mg/L HCPT (**c**), or control cells without any treatment (**d**). Apoptotic nuclei could be identified by their distinctively marginated and fragmented appearance under the fluorescent microscope. Bar: 20μm. **B.** Quantitative analysis of apoptotic cells after various treatments shown in ***A***. The bar graphs are the average results from three different experiments. * $P < 0.05$, compared to the control.

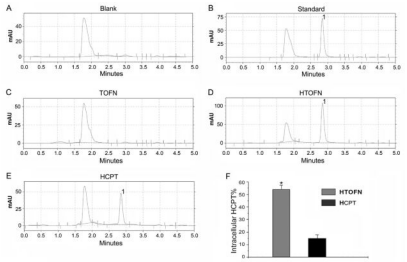

Figure 4.

Increased accumulation of HCPT in HCC827 cells treated with HTOFN. The amount of HCPT in the cells was analyzed by HPLC chromatographic spectrometry. **A.** Blank: the single peak represents the solvent. **B.** The HCPT standard solution was used to identify the HCPT peak position (**1**). **C.** The HPLC chromatographic spectrometry of TOFN. Since TOPN did not contain the drug, there is no HCPT peak. **D.** The HPLC chromatographic spectrometry of HTOFN contains HCPT peak (**1**). **E.** The HPLC chromatographic spectrometry of HCPT at the concentration that was loaded in HTOFN. **F.** Quantitative analysis of intracellular HCPT by calculating the concentration of HCPT obtained from HPLC divided by the concentration of HCPT used to treat cells. * $P < 0.05$, compared to the HCPT.

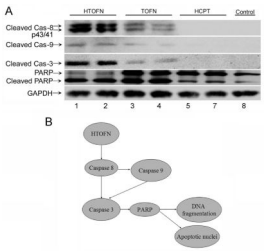

Figure 5.

A. Western blot analysis of cleaved caspases in HCC827 cells treated with HTOFN, TOFN, HCPT, or without treatment as a control. Lysates were prepared from the cells treated with 10 mg/L HTOFN, 10mg/L TOFN, or 8.6×10^{-2} mg/L HCPT. HCC827 cells without treatment were used as a control. The lanes of 2, 4, and 6 were the duplicates of lane 1, 3, and 5. The following antibodies were used: anti-cleaved caspase-8, anti-cleaved caspase-9, anti-cleaved caspase-3, and anti-PARP antibody. GAPDH was served as a loading control.

B. Schematic drawing showing HTOFN induced apoptosis in HCC827 cells. HTOFN activates caspase-8-dependent signaling pathway leading to cell apoptosis.

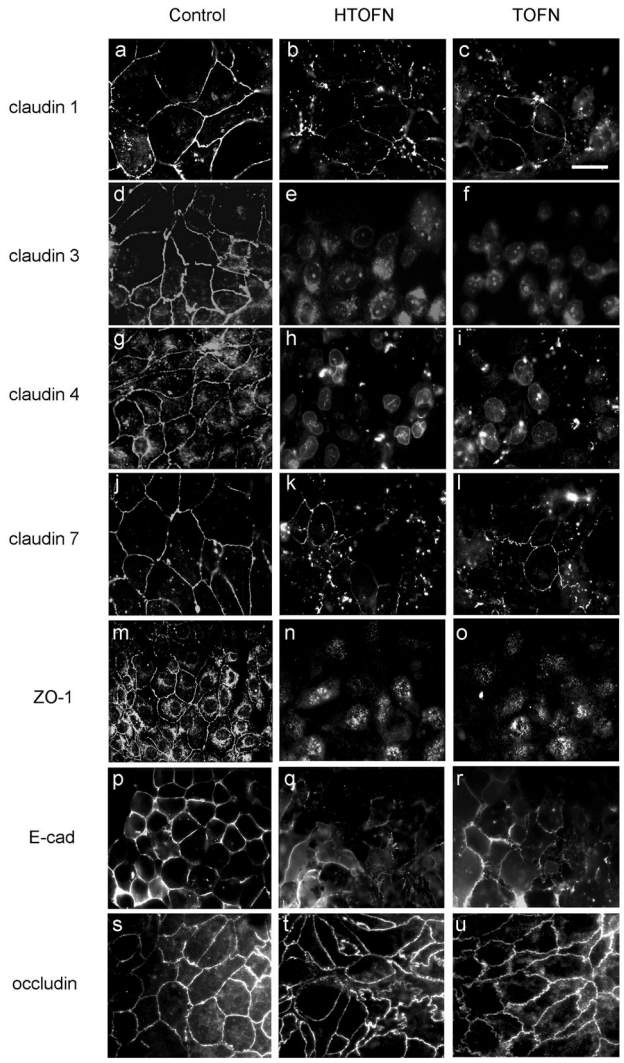

Figure 6.

Subcellular localization of cell junction proteins before and after treatments. The left column of images was taken from the control cells without any treatment. The middle and right columns of images were taken from the cells treated with either 10 mg/L HTOFN or 10mg/L TOFN for 24 h. The cells were fixed and immunostained with specific antibodies as indicated to the left of the columns. Bar: 20μm.

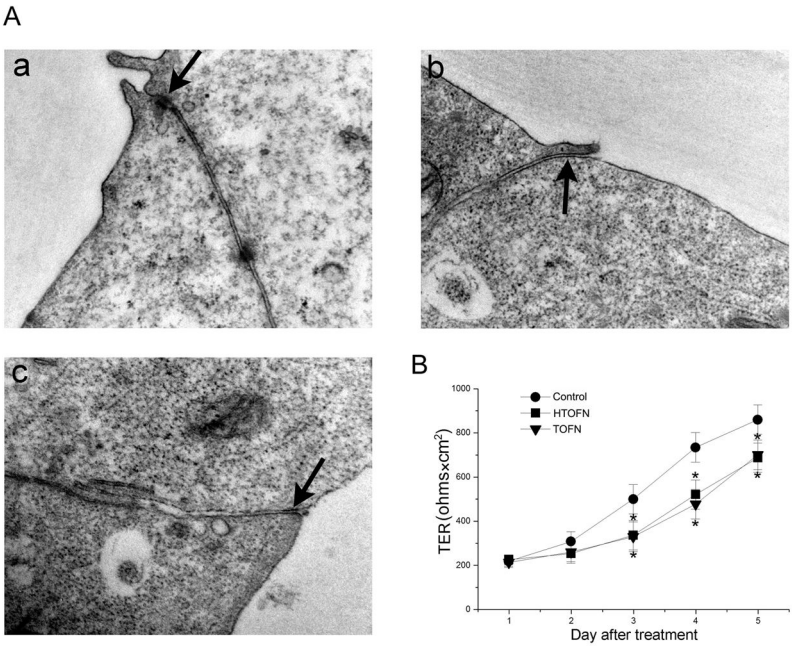

Figure 7.

Ultrastructural and functional examination of tight junctions in HCC827 cells. **A.** Transmission electron microscopic (TEM) images of HCC827 cells without any treatment (**a**), exposed to 10 mg/L HTOFN (**b**), or 10 mg/L TOFN (**c**) treatments for 48 h. The arrows in ***a–c*** indicate the tight junction area. Magnification: × 50,000. **B.** Decreased transepithelial electrical resistance (TER) after HTOFN and TOFN treatments. HCC827 cells were plated on Transwell plates and cultured for 7 days before they were treated with 10 mg/L HTOFN or 10 mg/L TOFN. TER was measured in the culture medium and determined as described in Methods. * $P < 0.05$, compared to the control.

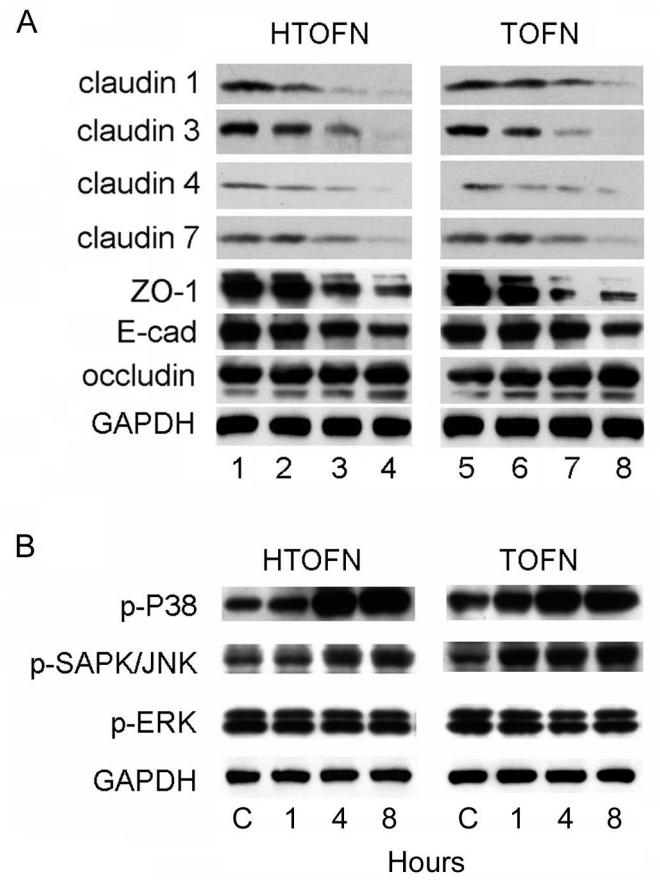

Figure 8.

Reduced expression levels of cell junction proteins and time-dependent activation of p38 MAP kinase and SAPK/JNK in HCC827 cells treated with HTOFN and TOFN. **A.** Lysates were prepared from HCC827 cells treated with HTOFN or TOFN (1, 5: control; 2, 6: 2.5 mg/L; 3, 7: 5 mg/L; 4, 8: 10 mg/L) for 48 h. HCC827 cells showed a dose-dependent decrease of expression levels of claudin-1, -3, -4, -7, ZO-1, and E-cadherin, but not occludin. **B.** Time-dependent increases of p38 and SAPK/JNK phosphorylation in HCC827 cells. HCC827 cell monolayers were incubated with 10 mg/L HTOFN or 10 mg/L TOFN for 1, 4, and 8 h.